International Journal of Green Energy

ISSN: 1543-5075 (Print) 1543-5083 (Online) Journal homepage: http://www.tandfonline.com/loi/ljge20

Comparison of ANN, MVR, and SWR models for computing thermal efficiency of a solar still

Ahmed F. Mashaly & A. A. Alazba

To cite this article: Ahmed F. Mashaly & A. A. Alazba (2016) Comparison of ANN, MVR, and SWR models for computing thermal efficiency of a solar still, International Journal of Green Energy, 13:10, 1016-1025, DOI: 10.1080/15435075.2016.1206000

To link to this article: http://dx.doi.org/10.1080/15435075.2016.1206000

Accepted author version posted online: 06 Jul 2016.
Published online: 06 Jul 2016.

INTERNATIONAL JOURNAL OF GREEN ENERGY
2016, VOL. 13, NO. 10, 1016–1025
http://dx.doi.org/10.1080/15435075.2016.1206000

Taylor & Francis
Taylor & Francis Group

Comparison of ANN, MVR, and SWR models for computing thermal efficiency of a solar still

Ahmed F. Mashaly[a] and A. A. Alazba[a,b]

[a]Alamoudi Chair for Water Researches, King Saud University, Riyadh, Saudi Arabia; [b]Agricultural Engineering Department, King Saud University, Riyadh, Saudi Arabia

ABSTRACT

In this paper, the viability of modeling the instantaneous thermal efficiency (η_{ith}) of a solar still was determined using meteorological and operational data with an artificial neural network (ANN), multivariate regression (MVR), and stepwise regression (SWR). This study used meteorological and operational variables to hypothesize the effect of solar still performance. In the ANN model, nine variables were used as input parameters: Julian day, ambient temperature, relative humidity, wind speed, solar radiation, feed water temperature, brine water temperature, total dissolved solids of feed water, and total dissolved solids of brine water. The η_{ith} was represented by one node in the output layer. The same parameters were used in the MVR and SWR models. The advantages and disadvantages were discussed to provide different points of view for the models. The performance evaluation criteria indicated that the ANN model was better than the MVR and SWR models. The mean coefficient of determination for the ANN model was about 13% and14% more accurate than those of the MVR and SWR models, respectively. In addition, the mean root mean square error values of 6.534% and 6.589% for the MVR and SWR models, respectively, were almost double that of the mean values for the ANN model. Although both MVR and SWR models provided similar results, those for the MVR were comparatively better. The relative errors of predicted η_{ith} values for the ANN model were mostly in the vicinity of ±10%. Consequently, the use of the ANN model is preferred, due to its high precision in predicting η_{ith} compared to the MVR and SWR models. This study should be extremely beneficial to those coping with the design of solar stills.

KEYWORDS

Artificial neural network; multivariate regression; solar desalination; step-wise regression

Introduction

The solar still desalination system offers a sustainable means for fresh water production. The solar still is one of the best solutions for solving the water problem. Its operation uses solar energy, which is clean, free and friendly to the environment. It can be easily fabricated with locally available materials and its operation is very simple. There is no need for hard maintenance or skilled personnel, resulting in few operational and maintenance costs. However, the widespread use of solar stills is often hindered by their relatively low productivity and low thermal efficiency compared to other desalination methods. Consequently, it has become necessary to increase the thermal efficiency and yield of solar still systems. In addition, accurate prediction of expected thermal efficiency and production is vital to the success of a solar desalination project, owing to the high capital costs involved. This leads to optimum capital costs and maximum the yield/production (Kabeel, Hamed, and Omara2012; Mashaly, Alazba, and Al-Awaadh 2016).

Many investigations have been carried out to improve and model the thermal efficiency and productivity of the still by various scientists and researchers (Sadineni et al. 2008; Vinoth and Bai 2008; El-Sebaii et al. 2009; Ahsan et al. 2010). However, experimental studies and thermal analysis of solar still desalination systems are complicated owing to numerous measurements and heat transfer processes required. Moreover, classical modeling methods, and heat and mass transfer models are very complex and require lengthy calculation for their solution. In addition, they are occasionally unreliable and need a large amount of data validation. As an alternative, an artificial neural network (ANN) was considered as a possible procedure that could use easily operational and meteorological data to precisely forecast still thermal efficiency (Facão, Varga, and Oliveira 2004).

ANNs are used in a wide variety of engineering applications. In the solar field alone, they have been used to calculate the performance parameters of flat-plate solar collectors (Kalogirou 2006), the modeling of a direct expansion solar assisted heat pump (Mohanraj, Jayaraj, and Muraleedharan 2008), predict the performance of a solar thermal energy system for hot water and space heating application (Yaïci and Entchev 2014), forecast the performance of a solar still (Santos et al. 2012; Mashaly et al. 2015; Mashaly and Alazba 2015), model solar energy potential (Ramedani, Omid, and Keyhani 2013), and model and analyze the productivity of solar desalination (Mousa and Gujarathi 2016).

Thermal efficiency is one of the most important parameters for judging the performance of solar stills since it details how effective the still is at absorbing solar energy and

CONTACT Ahmed F. Mashaly amashaly@ksu.edu.sa Chair for Water Researches, King Saud University, Riyadh, Saudi Arabia.
Color versions of one or more of the figures in the article can be found online at www.tandfonline.com/ljge.

evaporating and distilling water. It is one of the most effective elements in the solar desalination process and an essential tool for analyzing solar still performance (Yadav and Sudhakar 2015; Mashaly and Alazba 2016). Therefore, the objectives of this study are to: (1) develop a mathematical model to predict the thermal efficiency of a solar still using ANNs; (2) evaluate the performance of these ANNs using statistical comparison between predicted and experimental results, and; (3) compare the ANNs with the multivariate regression (MVR) and stepwise regression (SWR) models in terms of their suitability for predicting thermal efficiency.

Materials and Methods

Experimental Procedure

The experiments were conducted at the Agricultural Research and Experiment Station, at the Department of Agricultural Engineering, King Saud University, Riyadh, Saudi Arabia (24° 44'10.90"N, 46°37'13.77"E) between February and April 2013. The weather data were obtained from a weather station (model: Vantage Pro2; manufacturer: Davis, USA) close by the experimental site (24°44'12.15"N, 46°37'14.97"E). The solar still system used in the experiments was constructed from a 6 m^2single stage C6000 panel (F Cubed. Ltd., Carocell Solar Panel, Australia). The solar still panel was manufactured using modern, cost-effective materials such as coated polycarbonate plastic. When heated, the panel distilled a film of water that flowed over the absorber mat of the panel. The panel was fixed at angle of 29° from the horizontal plane. The basic construction materials were galvanized steel legs, an aluminum frame and polycarbonate covers. The transparent polycarbonate was coated on the inside with a special material to prevent fogging (patented by F Cubed, Australia). Cross-sectional view of the solar still is presented in Figure1.

The water was fed to the panel using centrifugal pump (model: PKm 60, 0.5 HP, Pedrollo, Italy) with a constant flow rate was 10.74 L/h. The feed was supplied by eight drippers/nozzles, creating a film of water that flowed over the absorbent mat. Underneath the absorbent mat was an aluminum screen that helped to distribute the water across the mat. Beneath the aluminum screen was an aluminum plate. Aluminum was chosen for its hydrophilic properties, to assist in the even distribution of the sprayed water. Water flowed through and over the absorbent mat, and solar energy was absorbed and partially collected inside the panel; as a result, the water was heated and hot air circulated naturally within the panel. First, the hot air flowed toward the top of the panel, then reversed its the direction to approach the bottom of the panel. During this process of circulation, the humid air touched the cooled surfaces of the transparent polycarbonate cover and the bottom polycarbonate layer, causing condensation. The condensed water flowed down the panel and was collected in the form of a distilled stream. Seawater was used as a feed water input to the system. The solar still system was run during the period from 02/23/2013 to 04/23/2013. Raw seawater was obtained from the Gulf, Dammam, in eastern Saudi Arabia (26°26'24.19"N, 50°10'20.38"E). The initial concentration of total dissolved solids (TDS), pH, density (ρ)and electrical conductivity (EC) of the raw seawater were 41.4 ppt, 8.02, 1.04 g.cm^{-3}, and 66.34 mS cm^{-1}, respectively. TDS and EC were measured using a TDS-calibrated meter (Cole-

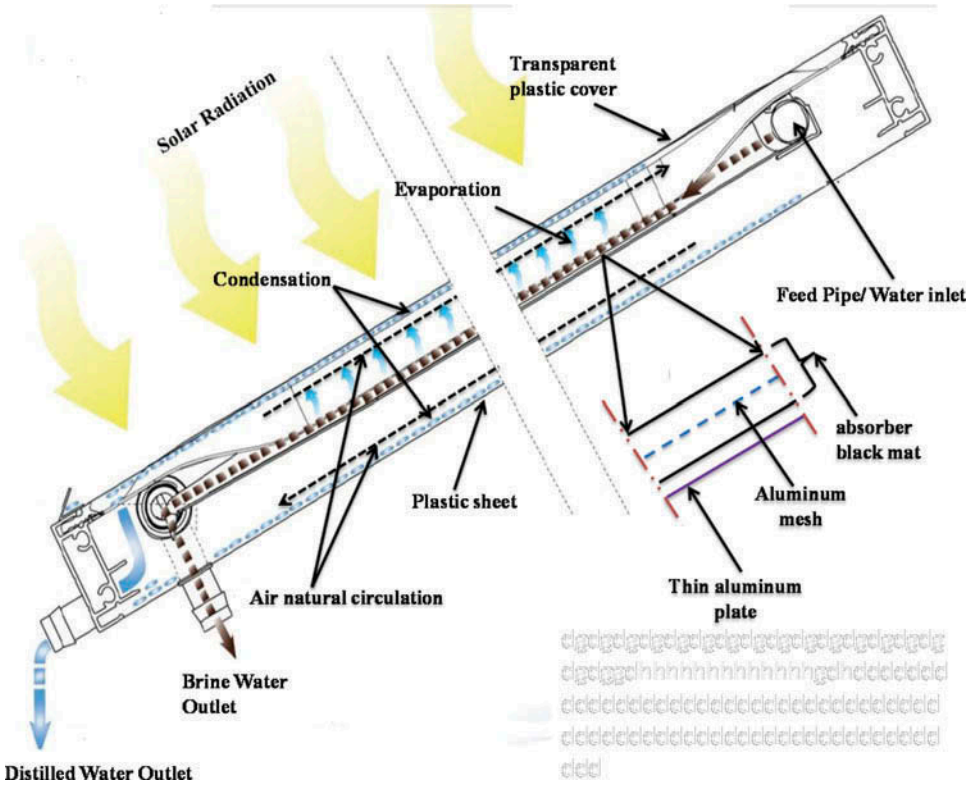

Figure 1. Cross-sectional view of the solar still used in the desalination process.

Parmer Instrument Co. Ltd., Vernon Hills, USA). A pH meter (model: 3510 pH meter, Jenway, UK) was used to measure pH. A digital-density meter (model: DMA 35_N, Anton Paar, USA) was used to measure ρ . The temperatures of the feed water (T_F) and brine water (T_B) were measured by using thermocouples (T-type, UK). Temperatures data for the feed and brine water were recorded on a data logger (model: 177-T4, Testo, Inc., UK) at 1 min intervals. The amount of feed water was measured by calibrated digital flow meter was mounted on the feed water line (micro-flo, Blue-White, USA). The amount of brine water and distilled water were measured by graduated cylinder. The seawater was fed separately to the panel using the pump described above. The residence time—the time taken for the water to pass through takes panel—was about 20 minutes. Therefore, the flow rates for the feed water, the distilled water and the brine water were measured every 20 minutes. Also, the total dissolved solids of feed water (TDS_F) and brine water (TDS_B) were measured every 20 minutes. The weather data such as air temperature (T_o), relative humidity (RH), wind speed (U) and solar radiation (Rs) were obtained from a weather station near the experimental site. In the experiment, there is one dependent variables which was the η_{ith} of solar desalination system and nine independent variables which are Julian day JD, T_o, RH, U, Rs, TDSF, TDSB,TF, and TB.

Computation of Thermal Efficiency for a Solar Still

The thermal efficiency of a solar still is defined as the amount of energy utilized to vaporize water in the still over the amount of incident solar energy on it . This is obtained by measuring the ratio of output energy to input energy. Output energy can be calculated by totaling the hourly condensate production, multiplied with the latent heat of vaporization. Input energy is the product of solar radiation within the area of the still. In this study the thermal efficiency of the solar still is expressed as instantaneous thermal efficiency (η_{ith})The η_{ith} of the solar still system can be computed using the following formula (Rahul and Tiwari 2009; Arunkumar et al. 2012).

$$\eta_{ith} = \frac{MD \times LHV}{Rs \times A} \times 100, \quad (1)$$

where, MD is the mass flow rate of distilled water during the time interval, kg/s

LHV: Latent heat of vaporization = 2275 kJ/kg
Rs: Solar Radiation, kW/m^2
A: Area of solar still, m^2

Artificial Neural Network Model (ANN)

ANN is a strong data modeling tool for capturing and representing complex input-output relationships. Due to its flexibility, the most commonly used ANN model is the multilayer perceptron; a network formed by simple neurons composed of input, output, and hidden layers. The perceptron computes a single output from multiple real-valued inputs by establishing combinations of linear relationships in accordance with input weights, and even nonlinear transfer functions. It is recommended that to use just one hidden layer be used since more layers worsen the problem of local minima (Zurada 1992; Hagan, Demuth, and Beale 1996; Dawson and Wilby 1998; Rai et al. 2005). The ANN model can be formulated mathematically as follows (Haykin 1999):

$$Y = F\left(\sum_{j=1}^{m} W_{kj}H_j + B_k\right), \quad (2)$$

$$H_j = F\left(\sum_{i=1}^{n} W_{ji}X_i + B_j\right), \quad (3)$$

where: W_{kj}= weights between hidden and output layers; W_{ji}= weights between input and hidden layers; H_j= neuron activation value; and X_i= input variables (JD, T_o, RH, U, Rs, T_F, T_B, TDS_F, and TDS_B); m is the number of neurons in the hidden layer; n is the number of neurons in the input layer; B_j and B_K and are the bias values for neurons in the hidden layer and output layer, respectively; F is the transfer function; and Y is the output (η_{ith}). This study used the sigmoid and hyperbolic tangent transfer functions, most commonly employed in the engineering field (Dawson and Wilby 1998; Zanetti et al., 2007).

Sigmoid transfer function (SIG) for any variable R:

$$F(R) = \frac{1}{1 + \exp(-R)}. \quad (4)$$

Hyperbolic tangent transfer function (TANH) for any variable R:

$$F(R) = \frac{1 - \exp(-2R)}{1 + \exp(-2R)}. \quad (5)$$

In this study, the ANN model was developed using the software package Qnet (Vesta Services 2000). The architecture of the ANN model used is shown in Figure 2. The modeling process includes three stages, namely, training, testing, and validation. The available data set, consisting of 160 data points obtained from experimental work, was divided randomly into training (70%), testing (20%), and validation (10%) subsets. Thus, the training, testing, and validation sets have 112, 32 and 16 data points, respectively. The most popular method of finding the optimal number of neurons in a hidden layer is by trial and error (Abutaleb 1991). Therefore, the trial and error technique was employed to determine the optimum neurons

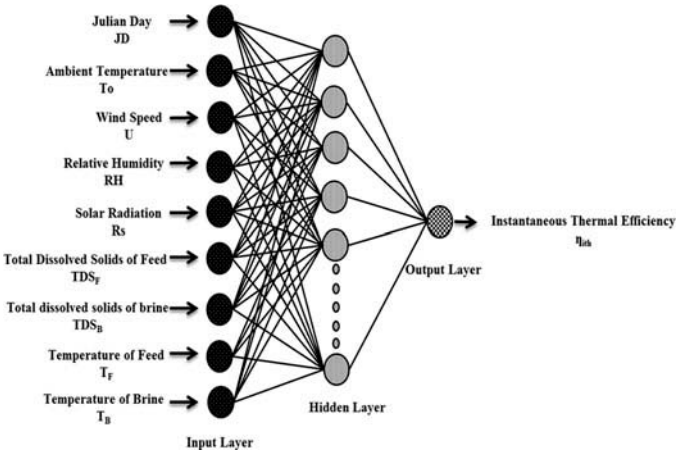

Figure 2. Architecture of the ANN model

in the hidden layer of the network. The data was applied after the normalization process between 0.15 and 0.85. The iteration was fixed to 200000. The learn rate and momentum factor were fixed at 0.01 and 0.8, respectively.

Multivariate Regression Model (MVR)

The MVR model is performed by considering more than one independent variable to achieve the best-fit equation between the input and output variables. Generally, the aim of MVR is to determine a relationship between input (independent variables) and output (dependent variable). The general form of the MVR model can be written as follows:

$$y = b_0 + b_1x_1 + b_2x_2 + b_nx_n, \tag{6}$$

where: y is the dependent variable, b_0;b_1;b_2;b_n are the regression parameter coefficients, and x_1;x_2;x_n are the independent variables (Mogaji 2016). In this study, the statistical package for Social Science (IBM SPSS statistics 22) program was used to develop the MVR model (SPSS Inc., Chicago, IL, USA). The MVR model was performed by the same experimental data used in the ANN model to form a mathematical relationship to forecast the η_{ith} (dependent variable) as a function of nine independent variables (JD, T_o, RH, U, Rs, T_F, T_B, TDS_F, and TDS_B).

Stepwise Regression Model (SWR)

The SWR is the step-by-step iterative construction of a regression model. The prediction model inputs are selected depending on their statistical significance. The independent variables are introduced into the model in the order determined by the strength of their association with the dependent variable to maximize its coefficient of determination R^2 (Card, Peterson, and Matson 1988). At each step of the selection, the p-value of an F-statistic is calculated to test models with and without a new predictor/independent variable. The F-statistic is formulated as follows:

$$F = \frac{\mathrm{RSS}_0 - \mathrm{RSS}_1}{\mathrm{RSS}_1/(n-k+1)}, \tag{7}$$

where: RSS_0 is the residual sum of squares in the original model without the additional new variable, RSS_1 is the residual sum of squares with the new variable included, n is the number of samples, and k is the number of variables present in the model.

Performance Evaluation Criteria

The performance of the models was evaluated using the following standard statistical performance evaluation criteria: coefficient of determination (R^2), root mean square error (RMSE), model efficiency (ME), overall index of model performance (OI), coefficient of residual mass (CRM), index of agreement (IA), performance index (PI), fractional bias (FB), mean absolute error (MAE), and mean absolute relative error (MARE):

$$R^2 = \frac{\left(\sum_{i=1}^{n}\left(x_{o,i}-\bar{x}_o\right)\left(x_{p,i}-\bar{x}_p\right)\right)^2}{\sum_{i=1}^{n}\left(x_{o,i}-\bar{x}_o\right)^2 \times \sum_{i=1}^{n}\left(x_{p,i}-\bar{x}_p\right)^2} \tag{8}$$

$$\mathrm{RMSE} = \sqrt{\frac{\sum_{i=1}^{N}\left(x_{o,i}-x_{p,i}\right)^2}{N}} \tag{9}$$

$$\mathrm{ME} = 1 - \frac{\sum_{i=1}^{n}\left(x_{o,i}-x_{p,i}\right)^2}{\sum_{i=1}^{n}\left(x_{o,i}-\bar{x}_o\right)^2} \tag{10}$$

$$\mathrm{OI} = \frac{1}{2}\left(1 - \left(\frac{\mathrm{RMSE}}{x_{\max}-x_{\min}}\right) + \mathrm{ME}\right) \tag{11}$$

$$\mathrm{CRM} = \frac{\left(\sum_{i=1}^{n}x_{p,i} - \sum_{i=1}^{n}x_{o,i}\right)}{\sum_{i=1}^{n}x_{o,i}} \tag{12}$$

$$\mathrm{IA} = 1 - \frac{\sum_{i=1}^{n}\left(x_{o,i}-x_{p,i}\right)^2}{\sum_{i=1}^{n}\left(\left|x_{p,i}-\bar{x}_o\right| + \left|x_{o,i}-\bar{x}_o\right|\right)^2} \tag{13}$$

$$\mathrm{PI} = \left[\left(\frac{\left(\sum_{i=1}^{n}\left(x_{o,i}-\bar{x}_o\right)\left(x_{p,i}-\bar{x}_p\right)\right)}{\sum_{i=1}^{n}\left(x_{o,i}-\bar{x}_o\right)\times\sum_{i=1}^{n}\left(x_{p,i}-\bar{x}_p\right)}\right) \times\left(1 - \frac{\sum_{i=1}^{n}\left(x_{p,i}-\bar{x}_p\right)^2}{\sum_{i=1}^{n}\left(\left|x_{p,i}-\bar{x}_p\right|+\left|x_{o,i}-\bar{x}_o\right|\right)^2}\right)\right] \tag{14}$$

$$\mathrm{FB} = \frac{2\left(\bar{x}_o - \bar{x}_p\right)}{\bar{x}_o + \bar{x}_p} \tag{15}$$

$$\mathrm{MAE} = \frac{\sum_{i=1}^{n}\left|x_{o,i}-x_{p,i}\right|}{n} \tag{16}$$

$$\mathrm{MARE} = \frac{1}{n}\left(\sum_{i=1}^{n}\left|\frac{x_{o,i}-x_{p,i}}{x_{o,i}}\right| \times 100\right) \tag{17}$$

where: $x_{o,i}$= observed value;$x_{p,i}$= predicted value;$x_{\min}$= minimum observed value;$x_{\max}$= maximum observed value; $\bar{x}_o$ = averaged observed values; $\bar{x}_p$ = averaged predicted values; and n = number of observations.

The R^2 can be utilized to determine the linear relationship between measured and predicted values (Bakirci 2009). In addition, R^2 measures the degree of correlation among the measured and predicted values with those close to 1.0 demonstrating good model performance. RMSE has the advantage of indicating and expressing an error in the same units as the parameter, thus, providing more information on the efficiency and accuracy of the model (Legates and McCabe 1999). The value of RMSE is always positive, and in an ideal case is equal to zero (Ma and Iqbal 1983). The lower the RMSE, the more accurate the performance of the model. For ideal data modeling, R^2 should approach1 as closely as possible, but the value of RMSE should be closer to zero. An ME value of 1.0 indicates a perfect fit between observed and predicted data, and this value can be negative. An ME value of 0 means that it is no better than a simple average model, since negative values show poor performance (Vanclay and Skovsgaard 1997; Zacharias, Heatwole, and Coakley 1996). The OI combines normalized RMSE and ME indicators to verify the mathematical

model performance. An OI value of 1 for a model indicates a perfect fit between the observed and predicted data (Alazba et al. 2012). The CRM parameter indicates the difference between observed and predicted data relative to the observe data. A zero value means a perfect fit. Positive values for the CRM indicate over prediction, while negative values indicate under prediction (League and Green 1991). The IA varies from 0.0 to 1.0. An IA value of 1 means a perfect fit, while0 shows no correlation (Willmott 1981). The PI varies from 0 to 1, and the closer PI is to 1, the better the model quality (Camargo and Sentelhas 1997). FB denotes the difference between the mean of predicted and observed values divided by their mean. FB varies between –2 and +2 with an optimal value of zero. Negative values show an over prediction of the model, while positive values indicate an under prediction (Cox and Tikvart 1990). MAE measures the average magnitude of errors in a set of forecasts, without considering their direction. MAE ranges from 0 to ∞, and its lower values imply high performance. MARE is used to assess the average difference between observed and predicted values. MARE expresses a percentage error. The closer MARE is to zero, the better the model performance.

Results and Discussion

Some statistical parameters of the raw data used with the ANN, MVR, and SWR models are given in Table 1. The average value of η_{ith} for the solar still system was 52.47%, and is consistent with the results of Omara, Kabeel, and Younes (2013), Abdullah (2013), and Yadav and Sudhakar (2015). In studying the effect of the TDS_F on solar distillation, the η_{ith} was found to decrease with the increase of TDS_F, which is in accordance with the results of Mahdi, Smith, and Sharif (2011) and Gnanadason et al. (2011). Moreover, it was revealed that the η_{ith} increased with an increase in Rs on the inclined surface, in agreement with the results of Singh et al. (1995) and El-Sebaii et al. (2009). More complete representations and descriptions of the experimental findings can be found in Mashaly, Alazba, and Al-Awaadh (2016).

ANN Model

The number of neurons in the hidden layer and transfer functions was varied to determine the ANN architecture. Table 2 shows the results of the statistical performance of the ANN model with a various number of neurons-nodes in the hidden layer and transfer functions. The neurons in the hidden layer were increased from 2 to 25 based on the trial and error technique. From Table 2, it can be seen that the best architecture for the ANN model has 12 neurons in the hidden layer. The SD, MXE, and CC for this configuration were: 1.147%, 3.035%, and 0.998, respectively (emboldened in Table 2). The average contributions of JD, T_o, RH, U, Rs, T_F, T_B, TDS_F, and TDS_B (inputs) to η_{ith} (output) were 9.11, 5.28, 10.58, 3.91, 10.81, 15.89, 12.92, 20.56, and 10.94, respectively (as shown in Table 2). Thus, the ANN model with one hidden layer and twelve neurons within it was selected as the optimum. The hyperbolic tangent (TANH) was the transfer function used in this model for the hidden and output layers. This function gave the best network performance and generally performed better than the sigmoid function (SIG), as shown in Table 2. Therefore, the developed ANN model architecture has a configuration of 9–12–1 neurons. This gave the best prediction of η_{ith} with the lowest error. The developed ANN model in Eq. (18) was used for predicting η_{ith} values, and can easily be programmed into a spreadsheet (i.e. Microsoft Excel) to predict the η_{ith} of the solar still.

$$\eta_{ith} = \frac{1 - \exp[(5.68F_1 + 4.83F_2 - 6.36F_3 - 6.34F_4 - 7.16F_5 - 3.17F_6 + 3.85F_7 + 1.83F_8 - 0.27F_9 - 4.44F_{10} + 6.48F_{11} + 7.52F_{12}) - 1.05]}{1 + \exp[(5.68F_1 + 4.83F_2 - 6.36F_3 - 6.34F_4 - 7.16F_5 - 3.17F_6 + 3.85F_7 + 1.83F_8 - 0.27F_9 - 4.44F_{10} + 6.48F_{11} + 7.52F_{12}) - 1.05]}, \quad (18)$$

where: the TANH function (Fj) used for this model is expressed as follows:

$$F_j = \frac{1 - \exp\left[-2\sum_{i=1}^{9}(W_{ji} \times X_i) - 2B_j\right]}{1 + \exp\left[-2\sum_{i=1}^{9}(W_{ji} \times X_i) - 2B_j\right]}, \quad (19)$$

where: the input parameters (X_i), connection weights (W_{ji}) and hidden biases (B_j) are listed in Table 3.

MVR Model

The obtained MVR model is expressed in Eq. (20) for predicting the η_{ith} values. The standard error of regression coefficients, *t*-stat, *p*-value, and independent variables are presented in Table 4. The significance of each coefficient in Eq. 20 was determined by the student's "t" test and *p*-value. From Table 4, the meaningfulness degrees of input variables can be seen. This degree of meaningfulness is determined via the value of p-value being *less than* 0.05. Larger *t*-values and smaller the p-values indicate a more significant corresponding coefficient. There is a significant relationship between the η_{ith} and RH, TDS_F and TDS_B. The standard errors of the coefficients in these variables are: 0.21%, 0.17%, and 0.16%, respectively. It can also be noted from Table 4 that JD, T_o, RH and TDS_F were inversely proportional to the η_{ith}. However, the R^2value of the developed MVR model was 0.856.

$$\eta_{ith} = 64.32 - 0.03 \times JD - 0.66 \times T_o - 0.43 \times RH + 0.51 \times U + 0.01 \times Rs + 0.49 \times T_F + 0.21 \times T_B - 1.46 \times TDS_F + 1.06 \times TDS_B \quad (20)$$

Table 1. Statistical Summary of the meteorological and operational parameters used in developing the ANN and MVR, and SWR models.

Input Parameters	AVG	MIN	MAX	SD	SE	CV
JD	74.92	54.00	113	23.22	1.84	0.31
T_o (°C)	26.64	16.87	33.23	3.68	0.29	0.14
RH (%)	23.36	12.90	70.00	12.90	1.02	0.55
U (km/h)	2.44	0.00	12.65	3.12	0.25	1.28
Rs (W/m^2)	587.55	75.10	920.69	181.93	14.38	0.31
T_F (°C)	36.66	22.10	42.35	4.27	0.34	0.12
T_B (°C)	49.58	27.59	68.69	8.16	0.64	0.16
TDS_F (PPT)	80.23	41.40	130.00	29.42	2.33	0.37
TDS_B (PPT)	95.54	46.20	132.8	29.59	2.34	0.31
η_{ith}(%)	52.47	15.84	82.16	17.65	1.40	0.34

AVG: average value, MIN: minimum value, MAX: maximum value, SE: standard error, SD: standard error, CV: coefficient of variation,

Table 2. Statistical performance of the ANN model with various node numbers in the hidden layer and transfer functions.

		Network Statistics			Average contribution of input node on output, %								
ANN	TF	SD	MXE	CC	JD	To	RH	U	Rs	T_F	T_B	TDS_F	TDS_B
9-2-1	SIG	4.733	13.522	0.964	8.41	13.06	10.64	8.15	4.79	8.96	4.78	24.75	16.46
	TANH	3.133	12.679	0.984	9.85	7.04	8.22	7.81	3.35	13.95	10.60	25.05	14.13
9-3-1	SIG	2.886	8.835	0.987	5.30	8.94	6.84	6.95	6.77	7.73	13.11	30.51	13.87
	TANH	2.721	8.566	0.988	12.32	7.99	8.65	7.27	7.62	13.64	7.91	22.05	12.53
9-4-1	SIG	2.515	8.495	0.990	10.19	5.80	10.48	6.26	5.05	13.68	10.44	24.09	14.00
	TANH	1.997	6.396	0.994	9.93	5.44	9.64	7.56	9.20	15.45	9.63	21.56	11.60
9-5-1	SIG	2.578	10.646	0.989	11.47	5.47	9.50	6.16	5.76	13.94	8.90	24.50	14.30
	TANH	2.135	6.579	0.993	9.45	6.98	10.55	4.45	6.47	15.37	12.33	22.49	11.92
9-6-1	SIG	2.220	6.845	0.992	10.03	4.14	9.59	5.78	6.75	14.74	12.33	23.55	13.10
	TANH	1.342	3.845	0.997	9.62	8.24	8.09	5.55	6.31	16.25	13.68	22.29	9.98
9-7-1	SIG	2.364	9.813	0.991	10.80	5.36	10.82	4.15	5.52	14.32	10.08	24.29	14.66
	TANH	1.634	4.252	0.996	8.04	6.80	8.13	4.74	10.67	13.62	15.08	20.07	12.85
9-8-1	SIG	2.379	8.214	0.991	10.13	6.21	11.03	5.06	4.71	13.65	11.81	24.61	12.77
	TANH	1.493	4.523	0.996	8.70	8.85	7.04	4.96	6.99	15.69	11.75	23.67	12.36
9-9-1	SIG	2.247	7.168	0.992	10.49	4.28	9.40	5.28	8.29	11.90	13.36	24.54	12.46
	TANH	1.436	4.715	0.997	9.56	6.65	8.20	4.58	9.52	13.25	15.54	22.70	9.99
9-10-1	SIG	2.209	8.069	0.992	10.44	5.48	11.67	3.86	5.58	13.96	12.47	24.85	11.70
	TANH	1.381	3.469	0.997	9.70	7.13	7.43	4.77	10.81	15.82	11.77	19.91	12.67
9-11-1	SIG	2.484	10.904	0.990	11.36	5.59	9.02	5.45	5.59	14.13	9.11	24.87	14.90
	TANH	1.390	5.378	0.997	7.08	7.90	9.22	5.33	10.66	9.92	14.10	24.89	10.91
9-12-1	SIG	2.466	11.206	0.990	13.10	4.77	10.97	2.93	5.06	14.95	8.87	25.01	14.34
	TANH	**1.147**	**3.035**	**0.998**	**9.11**	**5.28**	**10.58**	**3.91**	**10.81**	**15.89**	**12.92**	**20.56**	**10.94**
9-13-1	SIG	2.385	10.372	0.991	12.66	4.17	11.66	3.88	5.73	14.83	9.28	24.22	13.56
	TANH	1.265	4.172	0.998	9.58	6.42	10.01	4.57	12.87	12.89	13.35	20.27	10.04
9-14-1	SIG	2.343	10.393	0.991	10.66	4.87	11.48	4.70	6.39	14.33	9.85	23.94	13.78
	TANH	1.379	3.893	0.997	10.34	6.42	9.23	5.46	11.08	14.85	13.42	19.32	9.87
9-15-1	SIG	2.419	9.407	0.991	13.11	4.39	11.57	4.73	5.38	14.86	7.38	24.50	14.07
	TANH	1.086	3.870	0.998	9.11	4.59	11.76	4.31	12.82	15.59	12.52	19.80	9.49
9-16-1	SIG	2.090	7.693	0.993	11.30	5.38	9.53	5.14	8.04	13.95	10.56	22.96	13.13
	TANH	1.256	4.273	0.998	9.63	6.52	8.37	4.41	9.38	15.18	11.87	22.30	12.35
9-17-1	SIG	2.185	8.291	0.992	11.21	4.83	10.84	3.96	5.72	15.24	11.19	23.98	13.03
	TANH	1.120	4.052	0.998	9.86	5.39	12.18	3.69	8.39	16.80	11.71	22.00	9.98
9-18-1	SIG	2.200	7.093	0.992	10.53	3.77	8.16	5.24	7.35	14.09	13.10	24.11	13.64
	TANH	1.365	5.262	0.997	8.01	6.82	8.67	4.69	11.71	11.95	14.23	23.34	10.57
9-19-1	SIG	2.140	8.749	0.993	11.68	5.46	7.94	4.34	7.66	14.63	11.96	24.92	11.40
	TANH	1.321	4.783	0.997	9.27	8.70	8.36	5.09	9.99	15.11	12.85	20.29	10.33
9-20-1	SIG	2.227	8.650	0.992	10.71	4.92	10.07	5.05	6.12	14.06	10.85	24.54	13.68
	TANH	1.380	3.957	0.998	9.00	4.78	11.58	6.20	11.35	14.16	13.77	19.13	10.04
9-21-1	SIG	2.400	10.771	0.991	11.18	4.43	11.23	5.09	4.85	14.82	9.03	24.48	14.88
	TANH	1.366	4.655	0.997	9.86	5.10	8.60	3.76	11.31	15.70	14.36	20.61	10.70
9-22-1	SIG	2.471	10.519	0.990	12.75	5.22	8.19	4.98	5.61	14.27	9.30	25.34	14.35
	TANH	1.205	4.149	0.998	10.46	5.12	9.57	3.61	12.29	14.92	13.33	20.17	10.53
9-23-1	SIG	2.603	11.381	0.989	12.69	4.50	10.13	5.98	4.40	14.01	9.22	25.17	13.89
	TANH	1.200	3.101	0.998	10.48	5.70	11.80	3.56	11.28	14.58	12.86	19.75	9.98
9-24-1	SIG	2.259	7.509	0.992	10.53	5.13	8.11	6.56	5.29	13.97	12.23	24.42	13.77
	TANH	1.175	4.069	0.998	9.72	5.81	11.65	2.89	12.61	15.28	12.70	19.27	10.07
9-25-1	SIG	2.235	9.023	0.992	9.72	5.31	11.49	4.82	6.43	13.88	10.60	24.00	13.76
	TANH	1.165	4.691	0.998	9.06	5.57	9.31	4.26	12.96	14.66	13.86	20.03	10.30

TF: Transfer Function, SD: Standard Deviation, CC: Correlation Coefficient, MXE: Maximum Error.

Table 3. Weights (W_{ji}) and biases (B_j) between input and hidden layers for the developed ANN model.

	W_{ji}									
Hidden neurons (j)	JD	T_o	RH	U	Rs	T_F	T_B	TDS_F	TDS_B	β_j
1	1.068	−2.794	0.654	1.175	1.729	−0.83	0.531	1.606	−0.967	0.049
2	−0.547	1.319	0.507	0.919	0.199	−5.549	−1.639	2.657	0.964	0.861
3	0.389	0.343	1.043	−1.225	−1.237	−1.643	0.091	0.989	−1.443	0.601
4	1.874	−2.704	1.464	−0.081	−1.052	−2.081	3.52	−3.74	2.245	1.39
5	−1.788	−0.471	0.925	−1.696	1.535	1.224	−3.405	−2.017	3.328	−1.051
6	0.231	−0.385	1.45	0.176	0.485	−1.078	−1.015	0.314	1.169	−1.018
7	−0.359	−1.61	0.221	−1.386	1.369	0.383	1.496	−1.024	0.844	0.11
8	−0.476	−0.847	−0.127	0.416	−0.073	0.062	0.176	−0.208	0.14	−0.038
9	0.102	0.167	−0.019	−0.138	−0.211	−0.244	−0.292	−0.073	0.042	−0.312
10	0.023	1.149	1.864	0.307	1.58	−0.714	−0.517	−1.85	−1.427	1.252
11	−0.093	0.232	3.068	−0.706	−2.24	1.667	−2.247	−2.548	0.409	0.793
12	−1.384	0.883	−2.464	−2.221	1.823	−2.947	−0.458	0.898	1.278	0.246

Table 4. Standard error (SE) of regression coefficients, *t*-statistic (t-stat), and probability (*p*-value) of meteorological and operational parameters for the developed MVR models.

Dependent Parameters		Independent Parameters									
		Intercept	JD	T_o	RH	U	Rs	T_F	T_B	TDS_F	TDS_B
η_{ith}	SE	18.94	0.15	0.46	0.21	0.42	0.01	0.63	0.22	0.17	0.16
	t-stat	3.40	-0.23	-1.44	-2.06	1.21	0.8	0.77	0.94	-8.42	6.76
	p-value	0.00	0.82	0.15	0.04	0.23	0.42	0.44	0.35	0.00	0.00

SWR model

SWR models are developed by iteratively adding and removing the terms from a multilinear model based on their significance within a regression by using SPSS software. All nine dependent variables (JD, T_o, RH, U, Rs, T_F, T_B, TDS_F, and TDS_B) were used to create predicting models for η_{ith}. SWR produced four models with 1–4 predictor variables, where TDS_F was involved in each set of predictor variables, as listed in Table 5. It is clear that the variables of TDS_F and Rs have the most effect on η_{ith} modeling. The R^2 values associated with each of the five models ranged from 0.526 to 0.849. Corresponding standard errors of the estimate (SEE) ranged from 12.280% to 7.029%. It can be noted from Table 5 that the absence or presence of some of the input variables in the SWR models significantly affects the performance of these models. Model 1 with just the TDS_F performed worst, with R^2 = 0.526 and SSE = 12.280%. Model 2 performed better than Model 1, owing to the presence of Rs. The R^2 value of Model 2 was increased by 44.87% than that for Model 1. In addition, the SSE value of the Model 2 was decreased by 28.78% than that for Model 1. Following step 2 (Model 2), the accuracy was dramatically unchanged. However, Model 4 presented the best model for predicting η_{ith} (R^2 = 0.849, SEE = 7.029%), which involved Rs, TDS_F, TDS_B, and RH as predictor variables.

Comparison of the ANN, MVR, and SWR models

Figure 3 compares the predicted and observed η_{ith} values for the ANN, MVR, and SWR models using the training data sets. The data was mostly evenly distributed around the 1:1 line, showing very close visual agreement between observed values and predicted values for the ANN model. Table 6 shows the results of the statistical parameters, R^2, RMSE, ME, OI, CRM, IA, PI, FB, MAE, and MARE, which are numerical indicators used to evaluate the agreement between observed and predicted η_{ith}. From Table 6, it can be realized that the values of R^2, ME, OI, IA, and PI are high for the training data set computed from the ANN model, and low for the training data set computed from the MVR and SWR models. It can also be recognized that the statistical parameters RMSE and CRM have low values when η_{ith} is obtained through the ANN model, indicating good agreement with observed and predicted η_{ith} for the training data set. The CRM values are equal to 0.006, 0.004 and 0.003 for the ANN, MVR, and SWR models, respectively, meaning the values are over predicted. The OI value for the ANN model was closer to one than its value for the MVR and SWR models, and the CRM value for MVR and SWR was slightly closer to zero than for the ANN model during the training process. Also, the PI value for the ANN model was closer to one than its value for the MVR and SWR models. FB values for the ANN, MVR, and SWR models are negative, indicating over prediction; however the values are close to zero. For ANN, the MAE value (0.920%) was very close to zero. The value of MAE for the MVR and SWR models (5.421% and 5.615%) was almost six times that of the ANN model. The MARE value was 1.967% for the ANN model. The corresponding MARE values increased by about 478.90% and 517.49% for the MVR and SWR models, respectively. These results indicate that the ANN model can be used for η_{ith} modeling and is better than the MVR and SWR models in the training process.

Figure 4 shows the relative error for the ANN, MVR, and SWR models using the training data set. The figure indicates differences between the results of the three models with average relative errors of 0.67%, 2.23%, 2.32% for the ANN, MVR, and SWR models, respectively, using the training data set. It is clear that the values for the ANN model were lower than those of the MVR and SWR models, giving more accurate prediction values of η_{ith}.

The testing data set used for comparison indicated the R^2 values for MVR and SWR models were about 9.79% and -9.05%, respectively; less accurate than for the ANN model as shown in Table 6. It is clear from Figure 3 that the predicted η_{ith} values using the ANN model were in very good agreement with the observed η_{ith} values during the testing process. The RMSE value for the MVR and SWR models was about 1.62 and 1.58 times higher, respectively, than the value for the ANN model. However, the R^2, ME, OI,IA, and PI values are very close to one while RMSE, CRM, and FB values are close to zero, also indicating very good agreement between the experimental and predicted results from the ANN model during the testing process. The very small deviations between observed and predicted values in turn emphasize the effectiveness of the ANN in the prediction of η_{ith} values. The IA values for the MVR and SWR models are *slightly greater than* its value for the ANN model. The PI values for the ANN model were

Table 5. Equations representing stepwise regression models developed for estimating instantaneous thermal efficiency (η_{ith}).

Step	Equation	R^2	SEE (%)
1	$\eta_{ith} = 87.729 - 0.445\ TDS_F$	0.526	12.280
2	$\eta_{ith} = 65.982 - 0.503\ TDS_F + 0.046\ Rs$	0.762	8.745
3	$\eta_{ith} = 63.880 - 0.946\ TDS_F + 0.031\ Rs + 0.486\ TDS_B$	0.817	7.707
4	$\eta_{ith} = 66.358 - 1.313\ TDS_F + 0.020\ Rs + 0.935\ TDS_B - 0.421RH$	0.849	7.029

R^2: Coefficient of Determination; SEE: Standard Error of the Estimate

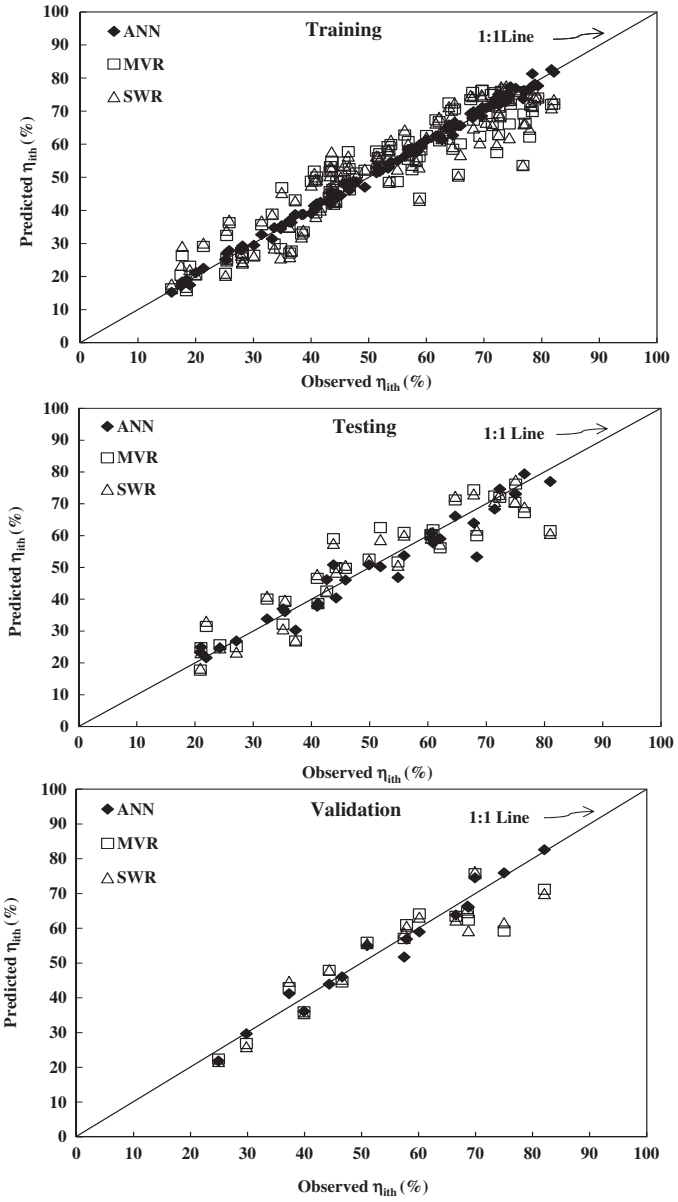

Figure 3. Comparison between observed and predicted values using the ANN, MVR, and SWR models during the training, testing, and validation processes.

8.10 % and 7.37% more accurate than that of the MVR and SWR models, respectively. The positive *value of the FB parameter for the ANN model indicated* an *under prediction, while* the negative *values of the FB parameter for the MVR and SWR models indicates*

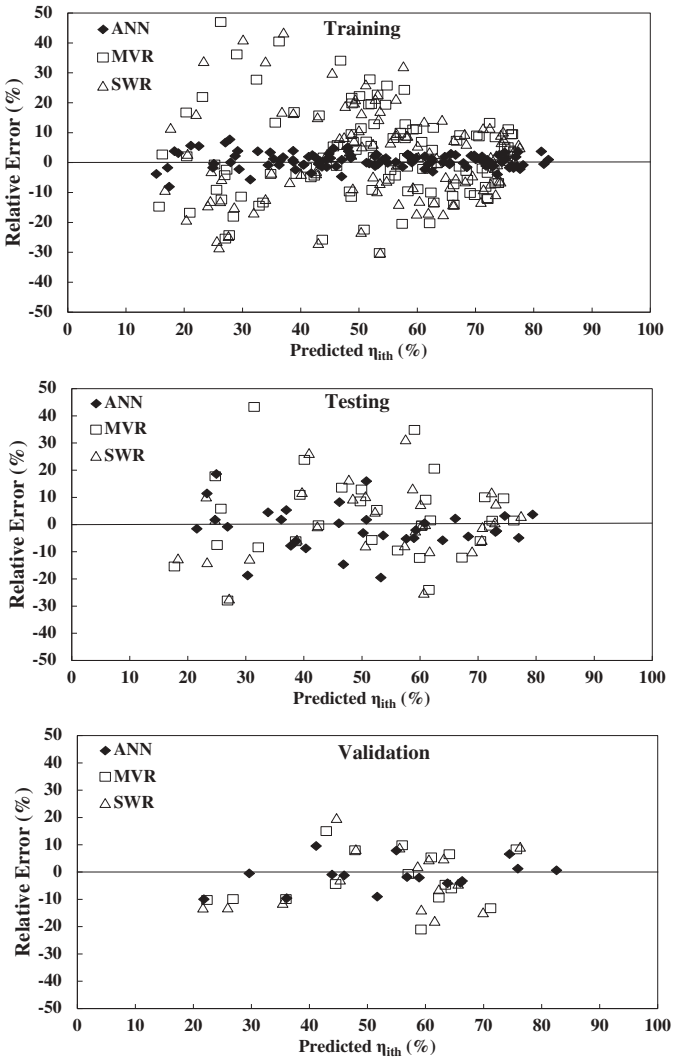

Figure 4. Relative errors for the ANN, MVR, and SWR models during the training, testing, and validation processes.

an *over prediction*. The values of MAE for the MVR and SWR models (5.123% and 4.971%) were almost double that of the ANN model. In addition, the values of MARE for the MVR and SWR models were nearly double that of the ANN model. The R^2, RMSE, ME, OI, CRM, IA, PI, FB, MAE, and MARE values confirm that MVR and SWR perform relatively poorly. *Figure 4* depicts the relative errors of predicted η_{ith} values for the testing data set for the ANN, MVR, and SWR models. Figure 4 illustrates that more than 81% of the errors fall in a domain ranging from + 10 to – 10 % for

Table 6. Statistical parameters for evaluating the performance of the ANN, MVR, and SWR models during Training, Testing, and Validation processes.

	R^2	RMSE	ME	OI	CRM	IA	PI	FB	MAE	MARE
Training										
ANN	0.996	1.147	0.996	0.989	0.006	0.999	0.997	–0.006	0.920	1.967
MVR	0.856	6.715	0.856	0.877	0.004	0.960	0.888	–0.004	5.421	11.387
SWR	0.849	6.873	0.849	0.873	0.003	0.958	0.882	–0.003	5.615	12.146
Testing										
ANN	0.950	4.169	0.945	0.938	–0.023	0.938	0.961	0.023	2.992	6.239
MVR	0.857	6.770	0.855	0.871	0.011	0.960	0.889	–0.011	5.123	11.471
SWR	0.864	6.574	0.864	0.877	0.007	0.963	0.895	–0.007	4.971	11.247
Validation										
ANN	0.971	2.897	0.968	0.959	–0.011	0.992	0.978	0.012	2.363	4.797
MVR	0.867	6.116	0.857	0.875	–0.029	0.960	0.894	0.029	4.951	8.904
SWR	0.857	6.321	0.847	0.868	–0.030	0.957	0.886	0.030	5.255	9.699

the ANN model. On the other hand, only about 56% of errors were in the vicinity of + 10 to – 10 for the MVR and SWR models.

Figure 3 shows the comparison between observed and predicted η_{ith} values for the ANN, MVR, and SWR models during the validation process, and shows very good agreement by the ANN model. Although there is also agreement by the MVR and SWR models, it is less accurate than for the ANN model. Figure 4 shows the relative errors of predicted η_{ith} values for the validation data set in the ANN, MVR, and SWR models. The relative errors of predicted η_{ith} values for the ANN model were mostly around ±10%. The average relative errors for the MVR and SWR models (-2.30% and -2.45%, respectively) were almost double that of the ANN model (-1.30%). Using the validation data set of the ANN model in the comparison shows that the MVR and SWR models had R^2values of about 11% and 12%, respectively; less accurate than that of the ANN model, as presented in Table 6. The values of RMSE for the MVR and SWR models (6.116% and 6.321%, respectively) were almost double that of the ANN model (2.897%). The ME, OI, and IA values for the ANN model were 13%, 10 %, and 3%, respectively; more accurate than that of the MVR model. Also, the ME, OI, and IA values for the ANN model were 15%, 11%, and 4%, respectively; more accurate than that of the SWR model. The PI value for the ANN model was closer to one than for the MVR and SWR models. The CRM and FB values for the MVR and SWR models were almost three times that of the ANN model. The MAE values of 4.951% and 5.255% for the MVR and SWR models were increased by 109.52% and 122.39%, respectively, compared to those of the ANN model. The MARE values in the ANN model were decreased by 46.13% and 50.54% than for the MVR and SWR models, respectively. These results indicate that the ANN model can be used effectively for η_{ith} modeling.

Table 6 and Figures 3 and 4 indicate that the ANN model performed better than the MVR and SWR models during the training, testing, and validation processes. According to the statistical criteria, the MVR and SWR models represented similar results, but the MVR provided better overall prediction accuracy. Based on the foregoing, the ANN model provides more accurate and reliable results than the MVR and SWR models. This agrees with the findings of other authors (Arulsundar, Subramanian, and Murth 2005; Nikolopoulos et al. 2007; Şahin, Kaya, and Uyar 2013; Citakoglu 2015; Mashaly and Alazba 2016).

Conclusions

The thermal efficiency of a solar still is the most important design assessment parameter, and in this study it is defined and expressed as instantaneous thermal efficiency (η_{ith}). The application of ANN, MVR, and SWR models on the experimental η_{ith} values of the solar still are compared and discussed. A wide range of parameters was considered for the formulation of the ANN model, which has nine input nodes, twelve hidden nodes, and one output neuron (i.e. a 9-12-1 node configuration). The nine input nodes are as follows: JD, T_o, RH, U, Rs, T_F, T_B, TDS_F, and TDS_B with η_{ith} being the sole output neuron. The same parameters were used to develop the MVR and SWR and these models were then trained, tested, and validated. The performance of the ANN, MVR, and SWR models were evaluated by comparing the predicted and experimental results, using standard statistical performance measures, namely R^2, RMSE, ME, OI, CRM, IA, PI, FB, MAE, and MARE. These comparisons revealed that agreement between the observed and predicted data was reasonable for the MVR and SWR models but better for the ANN model. The findings indicate that the ANN model has better performance than the MVR and SWR models, showing that the ANN modeling technique can be successfully used to predict the η_{ith} values of a solar still with very few errors. Accordingly, due to its precision, the ANN model is expected to be very useful in the design process of solar stills.

Nomenclature

ANN	artificial neural network
B_j	biases in the hidden layer
B_k	biases in the output layer
CC	correlation coefficient
CRM	coefficient of residual mass
CV	coefficient of variation
FB	fractional bias
IA	index of agreement
JD	Julian day
MAE	mean absolute error
MARE	mean absolute relative error
ME	coefficient of model efficiency
MVR	Multivariate regression
MXE	maximum error
OI	overall index of model performance
PI	performance index
R^2	coefficient of determination
RH	relative humidity
RMSE	root mean square error
Rs	solar radiation
SD	standard deviation
SE	standard error
SIG	sigmoid transfer function
SWR	Step-wise regression
TANH	hyperbolic tangent transfer function
T_B	temperature of brine water
TDS_B	total dissolved solids of brine water
TDS_F	total dissolved solids of feed water
T_F	temperature of feed water
T_o	ambient temperature
U	wind speed
W_{ji}	weights between input and hidden layers
W_{kj}	weights between hidden and output layers
x_{max}	minimum observed value
x_{min}	observed value
$x_{o,i}$	predicted value
$x_{p,i}$	averaged observed values
$\bar{\bar{x}}_0$	minimum observed value

Acknowledgment

The project was financially supported by King Saud University, Vice Deanship of Research Chairs.

References

Abdullah, A.S. 2013. Improving the performance of stepped solar still. *Desalination* 319:60–65.

Abutaleb, A.S. 1991. A neural network for the estimation of forces acting on radar targets. *Neural Networks* 4:667–678.

Ahsan A., K.M.S. Islam, T. Fukuhara, and A.H. Ghazali. 2010. Experimental study on evaporation, condensation and production of a new tubular solar still. *Desalination* 260(1–3):172–9.

Alazba, A. A., M. A. Mattar, M. N. ElNesr, and M. T. Amin. 2012. Field assessment of friction head loss and friction Correction factor equations. *Journal of Irrigation and Drainage Engineering* 138:166–176.

Arulsundar, N., N. Subramanian, and R.S.R. Murth. 2005. Comparison of artificial neural networks and multiple liner regression in optimization of formulation parameters of leuprlide acetate loaded leptosomes. *Journal of Pharmaceutical Sciences* 8:243–258.

Arunkumar, T., R. Jayaprakash, D. Denkenberger, A. Amimul, M. S. Okundamiya, T. S. k. Hiroshi, and H.Ş. Aybar. 2012. An experimental study on a hemispherical solar still. *Desalination* 286:342–348.

Bakirci, K. (2009). Correlations for estimation of daily global solar radiation with hours of bright sunshine in Turkey. *Energy* 34:485–501.

Camargo, A.P., and P.C. Sentelhas.1997. Performance Evaluation of Different Potential Evapotranspiration Estimating Methods in the State of São Paulo, Brazil. *Revista Brasileira de Agrometeorologia***5**:89–97.

Card, D.H., D.L. Peterson, and P.A. Matson. 1988. Prediction of leaf chemistry by the use of visible and near infrared reflectance spectroscopy. *Remote Sensing of Environment* 26(2):123–147.

Citakoglu, H. 2015. Comparison of artificial intelligence techniques via empirical equations for prediction of solar radiation. *Computers and Electronics in Agriculture* 118:28–37.

Cox, W.M., and J.A. Tikvart. 1990. A statistical procedure for determining the best performing air quality simulation model. *Atmospheric Environment*. 24A:2387–2395.

Dawson, W.C., and R. Wilby. 1998. An artificial neural networks approach to rainfall-runoff modelling. *Hydrological Sciences Journal* 43 (1):47–66.

El-Sebaii A., A. Al-Ghamdi, F. Al-Hazmi, and A. S. Faidah. 2009. Thermal performance of a single basin solar still with PCM as a storage medium. *Applied Energy* 86(7–8):1187–95.

Facão, J., S. Varga. and A. C. Oliveira.2004. Evaluation of the use of artificial neural networks for the simulation of hybrid solar collectors. *International Journal of green Greenenergy*1(3):337–352.

Gnanadason, M. K., P. S. Kumar, G. Sivaraman, and J. E. S. Daniel. 2011. Design and performance analysis of a modified vacuum single basin solar still. *Smart Grid and Renewable Energy*2(4):388–395.

Hagan, M. T., H.B. Demuth, and M.H. Beale. 1996. *Neural Network Design*, Boston, Massachusetts: PWS Publishing Company.

Haykin, S. 1999. *Neural Networks. A Comprehensive Foundation*. New Jersey: Prentice Hall International Inc.

Kabeel, A.E., M.H. Hamed, and Z.M. Omara.2012. Augmentation of the basin type solar still using photovoltaic powered turbulence system. *Desalination and Water Treatment* 48:182–190.

Kalogirou, S.A. 2006. Prediction of flat-plate collector performance parameters using artificial neural network. *Solar Energy* 80:248–259.

Legates, D.R., and J. McCabe. 1999. Evaluating the use of "goodness-of fit" measures in hydrologic and hydro climatic model validation. *Water Resources Research* 35:233–241.

Loague, K., and R.E. Green. 1991. Statistical and graphical methods for evaluating solute transport models: Overview and application. *Journal of Contaminant Hydrology* 7:51–73.

Mahdi, J.T., B.E. Smith, and A.O. Sharif. 2011. An experimental wick-type solar still system: Design and construction. *Desalination* 267:233–238.

Mashaly, A. F., and A. A. Alazba. 2015. Comparative investigation of artificial neural network learning algorithms for modeling solar still production. *Journal of Water Reuse and Desalination*5(4): 480–493.

Mashaly, A. F., A. A. Alazba, A. M. Al-Awaadh, and M. A. Mattar. 2015. Predictive model for assessing and optimizing solar still performance using artificial neural network under hyper arid environment. *Solar Energy*118:41–58.

Mashaly, A. F., A. A. Alazba, and A. M. Al-Awaadh. 2016. Assessing the performance of solar desalination system to approach near-ZLD under hyper arid environment. *Desalination and Water Treatment* 57:12019–12036.

Mashaly, A. F., and A.A. Alazba. 2016. MLP and MLR models for instantaneous thermal efficiency prediction of solar still under hyper-arid environment. *Computers and Electronics in Agriculture* 122:146–155.

Mogaji, K. A. 2016. Geoelectrical parameter-based multivariate regression borehole yield model for predicting aquifer yield in managing groundwater resource sustainability. *Journal of Taibah University for Science* 10:1658–3655.

Nikolopoulos, K., P. Goodwin, A. Patelis, and V. Assimatopoulos. 2007. Forecasting with cue information: A comparison of multiple regressions with alternative forecasting approaches. *European Journal of Operational Research* 180:354–368.

Omara, Z.M., A.E. Kabeel, and M.M. Younes. 2013. Enhancing the stepped solar still performance using internal reflectors. *Desalination* 314:67–72.

Rahul, D. and G.N. Tiwari. 2009. Characteristic equation of a passive solar still. *Desalination*245:246–65.

Rai, P., G. C. Majumdar, S. DasGupta, and S. De. 2005. Prediction of the viscosity of clarified fruit juice using artificial neural network: A combined effect of concentration and temperature. *Journal of Food Engineering* 68:527–533.

Sadineni, S.B., R. Hurt, C.K. Halford, and R.F. Boehm. 2008. Theory and experimental investigation of a weir-type inclined solar still. *Energy* 33 (1):71–80.

Şahin, M., Y. Kaya, and M. Uyar. 2013. Comparison of ANN and MLR models for estimating solar radiation in Turkey using NOAA/AVHRR data. *Advances in Space Research* 51(5):891–904.

Santos, N. I., A. M. Said, D. E. James, and N. H. Venkatesh. 2012. Modeling solar still production using local weather data and artificial neural networks. *Renewable Energy* 40:71–79.

Singh, A.K., G.N. Tiwari, P.B. Sharma, and E. Khan. 1995. Optimization of orientation for higher yield of solar still for a given location. *Energy Conversion and Management* 36:175–187.

Vanclay, J.K., and J.P. Skovsgaard. 1997. Evaluating forest growth models. *Ecological Modelling* 98:1–12.

Vesta Services Inc. 2000. Qnet2000 Shareware, Vesta Services, Inc., 1001 Green Bay Rd, STE 196, Winnetka, IL 60093.

Vinoth, K.K., and R. K. Bai. 2008. Performance study on solar still with enhanced condensation. *Desalination* 230 (1–3):51–61.

Willmott, C.J. 1981. On the validation of models. *Physical Geography* 2:184–194.

Yadav, S., and K. Sudhakar. 2015. Different domestic designs of solar stills: A review. *Renewable and Sustainable Energy Reviews* 47:718–731.

Yaïci, W., and E. Entchev. 2014. Performance prediction of a solar thermal energy system using artificial neural networks. *Applied Thermal Engineering* 73:1348–1359.

Zacharias, S., C.D. Heatwole, and C.W. Coakley. 1996. Robust quantitative techniques for validating pesticide transport models. *Transactions of the ASAE* 39:47–54.

Zanetti, S.S., E.F. Sousa, V.P.S. Oliveira, F.T. Almeida, and S. Bernardo. 2007. Estimating evapotranspiration using artificial neural network and minimum climatological data. *Journal of Irrigation and Drainage Engineering—ASCE* 133 (2): 83–89.

Zurada, J. M. 1992. *Introduction to Artificial Neural Systems*. Saint Paul, Minnesota, West Publishing Company.